THE NEW ZGS INJECTOR PROPOSAL

Rolland Perry
Argonne National Laboratory

The history of accelerators shows that as each one becomes operational and as new experiments are designed, there is an ever increasing demand for higher beam intensity or higher energy, or both. The ZGS is no exception to this rule. Consequently, we are presently considering an improvement program for the ZGS which includes (a) a new 200 MeV, high intensity injector system, (b) remodeling of the ZGS rf system to accommodate larger beams, (c) rebuilding of the ZGS inner vacuum chambers to withstand full atmospheric pressure and to eliminate the likelihood of radiation damage, and (d) provisions for remote handling of targetry and other highly radioactive components in the ZGS.

I shall discuss only the proposed injector system.

In the early planning of the Zero Gradient Synchrotron (ZGS), it was conservatively estimated that a 50 MeV linac could be expected to inject into the ZGS a proton beam of about 5 mA with pulse lengths of about 200μsec. This would give about 6×10^{12} protons per pulse; and assuming a capture efficiency of 50% for the ZGS, the latter should then be able to accelerate about 3×10^{12} protons per pulse to full energy. As this was nearly two orders of magnitude higher than the achievements of any then existing proton synchrotron, it was expected that the ZGS would be in a very favorable position with respect to beam intensity for some time after its completion.

When the parameters for the ZGS were finalized, the space-charge limit was determined to be about 2.6×10^{13} protons per pulse after bunching for a 50 MeV injected beam.[1] To reach this level would require an injected beam of 50 mA from the linac. Up to the present time the 50 MeV linac has injected 17 mA into the ZGS. Presumably, with careful adjustment of all parameters, 50 mA might be achieved with the rf power available. This will bring the injected beam approximately to the space-charge limit of the ZGS.

Consideration of how it might be possible to increase the output of the ZGS beyond the inherent existing space-charge limit led to the realization that increase of the injection energy would push the space-charge limit to a higher level and thus permit acceleration of a larger number of particles per pulse. Furthermore, increasing the energy of the injected beam will reduce its angular divergence and thus permit injecting through a

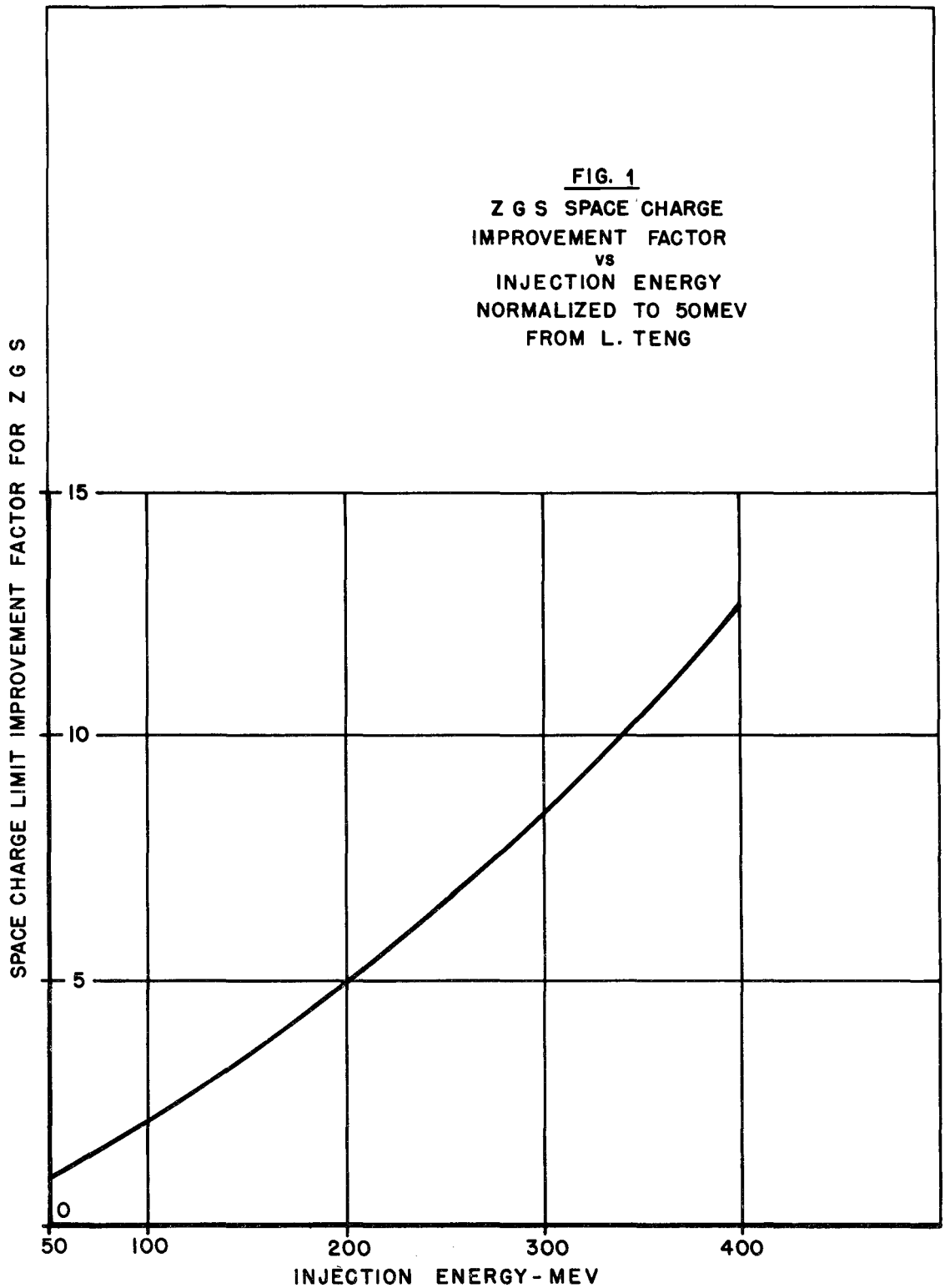
FIG. 1
Z G S SPACE CHARGE
IMPROVEMENT FACTOR
VS
INJECTION ENERGY
NORMALIZED TO 50MEV
FROM L. TENG
SPACE CHARGE LIMIT IMPROVEMENT FACTOR FOR Z G S
15
10
5
0
50
100
200
300
400
INJECTION ENERGY - MEV

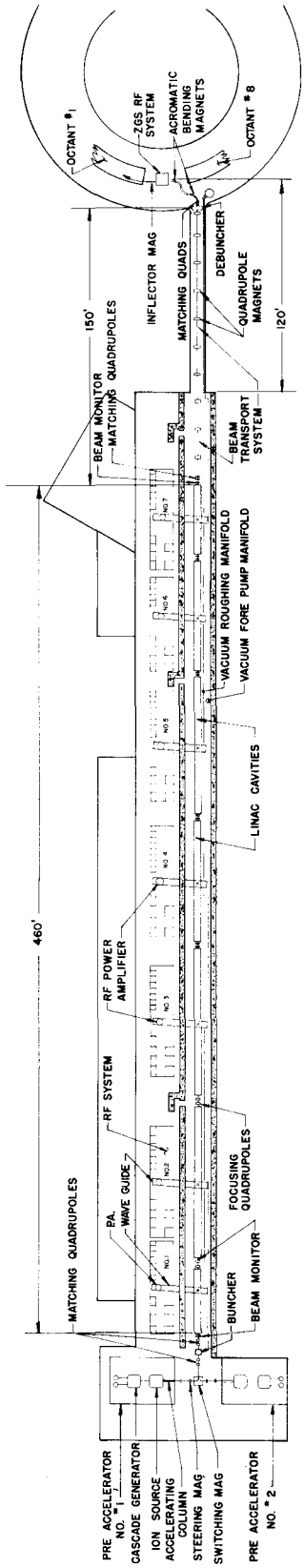

FIG. 2
200 MeV INJECTOR SYSTEM FOR THE
ZERO GRADIENT SYNCHROTRON

smaller aperture into the ZGS, with the consequence that, by decreasing the rate of rise of the ZGS guide field, the injection time can be increased to about 400 μ sec.

The space-charge limit of the ZGS at injection increases with injection energy somewhat more rapidly than linearly, as shown in Fig. 1 up to 400 MeV.

However, as the intensity of an accelerator rises, shielding requirements also increase. The safe limit of intensity for the ZGS basic shielding is believed to be about 10^{14} particles per pulse, which imposes a practical upper limit on injection energy.

Choosing an injection energy of 200 MeV provides an increase in the ZGS space-charge limit by a factor of five above the limit at 50 MeV, which would just about match the limit of the basic shielding.

The proposed injector system is comprised of the following major components shown in Fig. 2.

A 750 keV preaccelerator, including an ion source and ion focusing and accelerating elements.

A beam transport system and beam analysis system for the 750 keV ion beam.

An ion buncher for phase bunching of the ion beam.

A 200 MeV linear accelerator, comprised of seven or eight separate cavities, each driven by a high-powered rf amplifier and all properly phased together and locked to a common rf oscillator.

A beam analyzing and beam transport system for the 200 MeV proton beam.

A set of achromatic deflecting magnets to conduct the proton beam into the Zero Gradient Synchrotron and place it on its proper orbit.

It is planned to inject the 200 MeV beam into the ZGS at the No. 1 straight section but along a beam line which will permit building and testing the new system completely, except for the beam transport and debuncher portion, before disturbing the existing system. It is expected that a period of three years will be required for construction and testing and about six months for installation of the connecting equipment and modifications to the ZGS equipment.

Two complete preaccelerators are planned in order to reduce the probability of down time of the ZGS facility due to ion source or other pre-accelerator problems. The beam switching magnet will permit use of either preaccelerator beam for injection. At the same time the beam from the other preaccelerator could be deflected in the opposite direction for beam analysis, etc.

The parameters selected for the preaccelerator are as follows:

Beam energy	750 keV $\pm$ 0.1%
Peak proton beam current	200 mA
Beam pulse duration	400 - 800 μsec.
Pulse repetition rate	5 - 10 per sec.
Beam emittance	10 π - 17 π cm-mr.

An ion source development program is presently under way, including investigation of the Russian plasma expansion cup idea. Also, in co-operation with MURA personnel, plans are being made for testing short accelerating column designs, with the hope of attaining improved beam quality by use of rapid acceleration in a controlled field configuration.

The beam from the preaccelerator will be focused through the apertures of a multiple-harmonic buncher by a set of quadrupole magnets and will be matched into the first cavity of the linac by another set of quadrupole lenses. Beam pulse transformers, Faraday cups, and beam-defining slits will be placed appropriately along the beam path to permit amplitude and beam quality measurements ahead of the linac. An electro-static deflection type fast beam chopper will also be placed ahead of the linac.

Because the linac is to serve the ZGS with high efficiency, the parameters chosen should be such as to meet all the minimum require-ments without imposing stress on any components. The following param-eters are based on this basic philosophy.

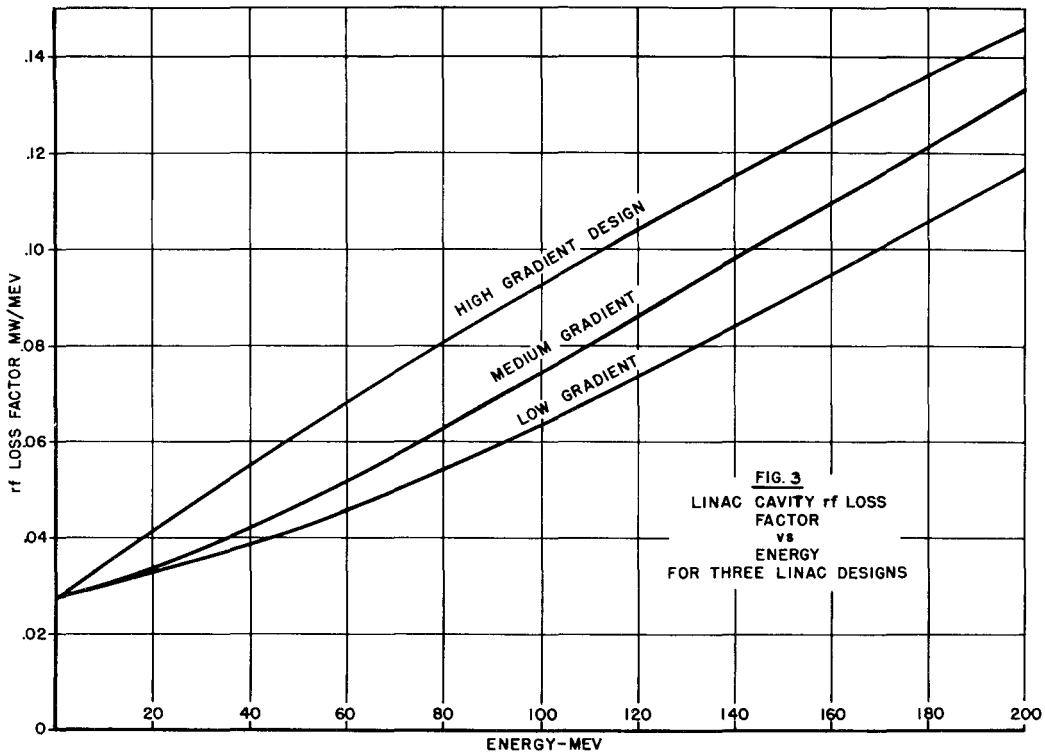

FIG. 3
LINAC CAVITY rf LOSS FACTOR vs ENERGY FOR THREE LINAC DESIGNS

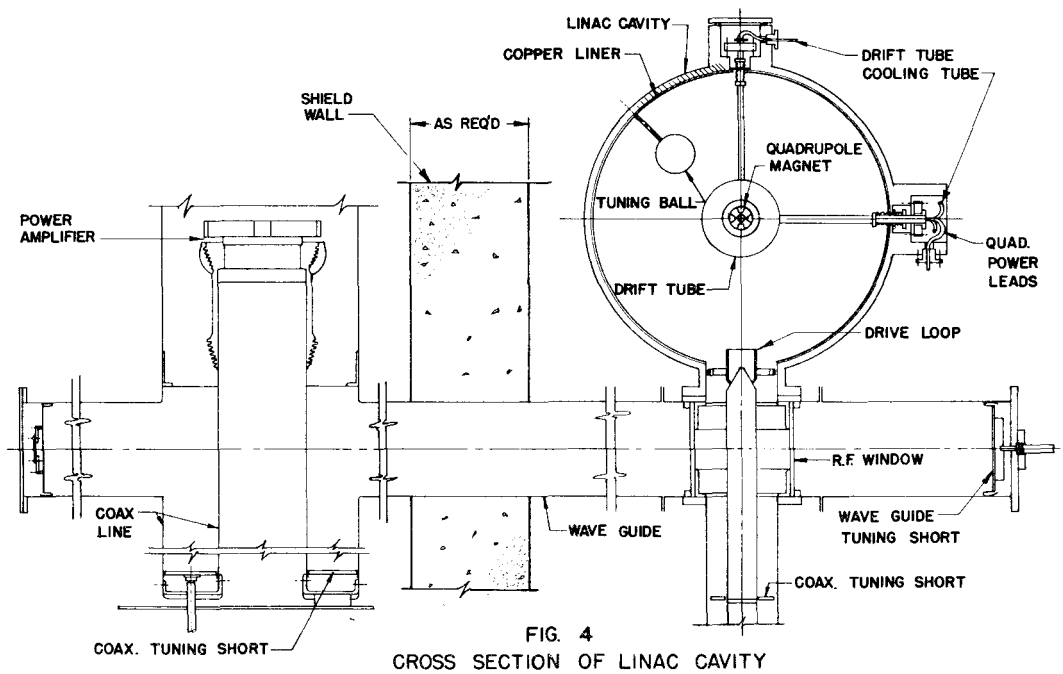

FIG. 4
CROSS SECTION OF LINAC CAVITY

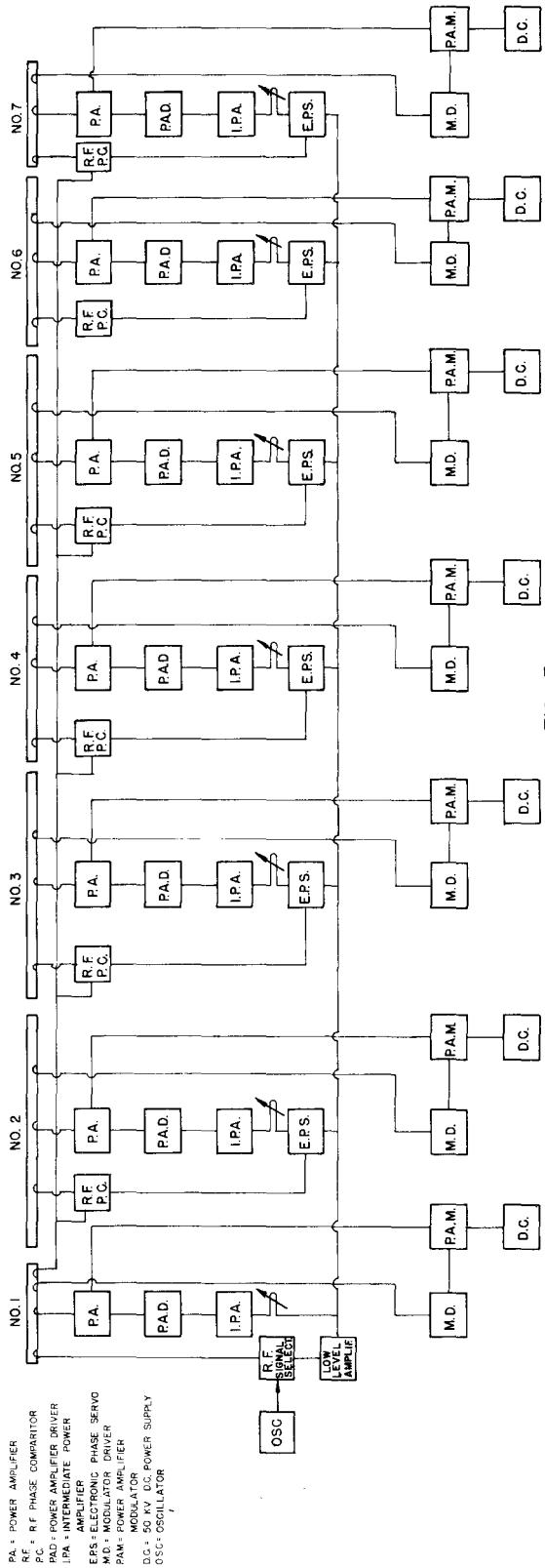

FIG. 5 BLOCK DIAGRAM OF THE R.F. SYSTEM FOR THE 200 MeV LINAC

Linac Parameters

Item	Value
Number of Cavities	7 - 8
Input Energy	750 keV
Final Energy	200 MeV
Input Current (protons)	150 mA
Output Current	100 mA
Transverse Phase Acceptance	17π cm-mr
Output Beam Emittance	4.6π cm-mr
Repetition Rate	5 per sec
Beam Pulse Length	400 - 500 μsec
RF Pulse Length	1000 μ sec
RF Duty Factor	0.5%
RF Losses in Cavities	17 MW
RF Power for Beam Acceleration	16 MW
Temperature Stability	$< \pm 0.25^{\circ}$ C

The linac will be comprised of seven[2] separate cavities, each powered by a single rf amplifier capable of at least 5 MW peak rf power. The parameters of each cavity will be so chosen as to give the most efficient division of rf power, P_n, between cavity losses and beam power at the design beam current, I. The incremental energy gain, ΔW_n, for the n^{th} cavity when this condition is satisfied is given by

$$\Delta W_n = \frac{P_n}{L_n + I} \quad \text{(MeV)}$$

where $L_n \equiv$ average rf losses/MeV in the n^{th} cavity.

The rf loss factor, L_n, is a function of drift tube and cavity geometry. For a given cell it increases with drift tube diameter. It also increases with energy since drift tube lengths must increase with energy. It is also proportional to the square of the mean rf gradient, E_o, in the cavity. Figure 3 shows the general behavior of this factor as a function of energy for three different 200 MeV linac designs computed by MURA personnel who are cooperating with ANL in the design of the linac.

The linac cavities will be much like the present 50 MeV cavity. A cross section through the cavity and drive line is shown in Fig. 4. RF power from a power amplifier is coupled via a coax transition into a rectangular wave guide. At the linac end of the wave guide, power is

coupled through a cylindrical ceramic window into a short coaxial line which is terminated by a coupling loop at the linac cavity. The loop penetration is adjustable, and irises in the wave guide, together with tuning shorts at the ends of both wave guide and coax lines, permit impedance matching.

Drift tubes will be of the cylindrical type, which MURA people have computed, because of the simplicity of this design and the resultant economy of fabrication. However, the drift tubes for the first cavity may be of the Christofilos type, used in the existing injector, because the computer program is not yet capable of giving reliable results below 20 MeV. A dc quadrupole magnet will be installed in each drift tube although they may not all be necessary at the high energy end.

The type of tuner has not been established although ball tuners similar to those in the existing linac are being considered. It is believed from our experience in setting up the field distribution in the 50 MeV linac that a tuner in each cell may be very desirable, and this is presently being planned. For slow servo tuning of an entire cavity, an eccentric bar running along the cavity wall offers an interesting possibility.

Each of the cavities of the linac must be driven at the same rf frequency, and each must have the proper phase and amplitude. Because of the relatively large beam loading expected and the variation of cavity shunt impedance with energy, amplitude control must be either preprogrammed or servo controlled. Phasing also will require fast servo control.

The rf system is shown in block diagram form in Fig. 5. Each of the amplifier chains will be identical in operational requirements, and each will be separately controllable. The following table lists the specific requirements of the system.

Performance Specifications for the 200 MeV Linac RF System

Item	Value
Operating Frequency	201.25 Mc/sec
Pulse Length, Variable to	700 - 1000 μsec
Pulse Repetition Rate, Variable to	0.5 - 5 per sec
RF Duty Factor	0.035% - 0.5%
Number of Power Amplifiers	7 - 8
Peak RF Power per Amplifer	5 MW
Total Peak RF Power	33 - 37 MW

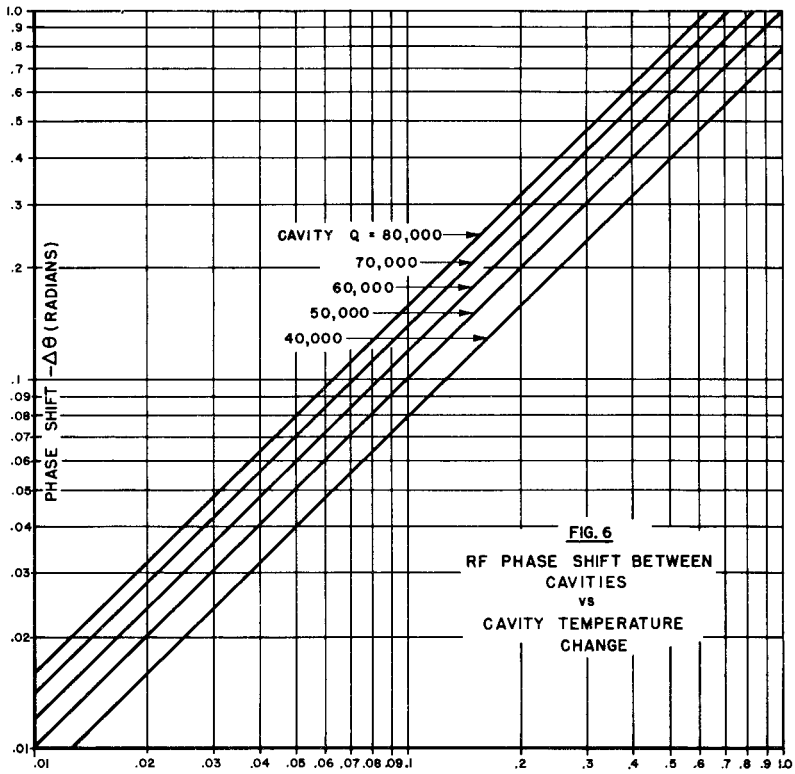

FIG. 6
RF PHASE SHIFT BETWEEN CAVITIES
vs
CAVITY TEMPERATURE CHANGE

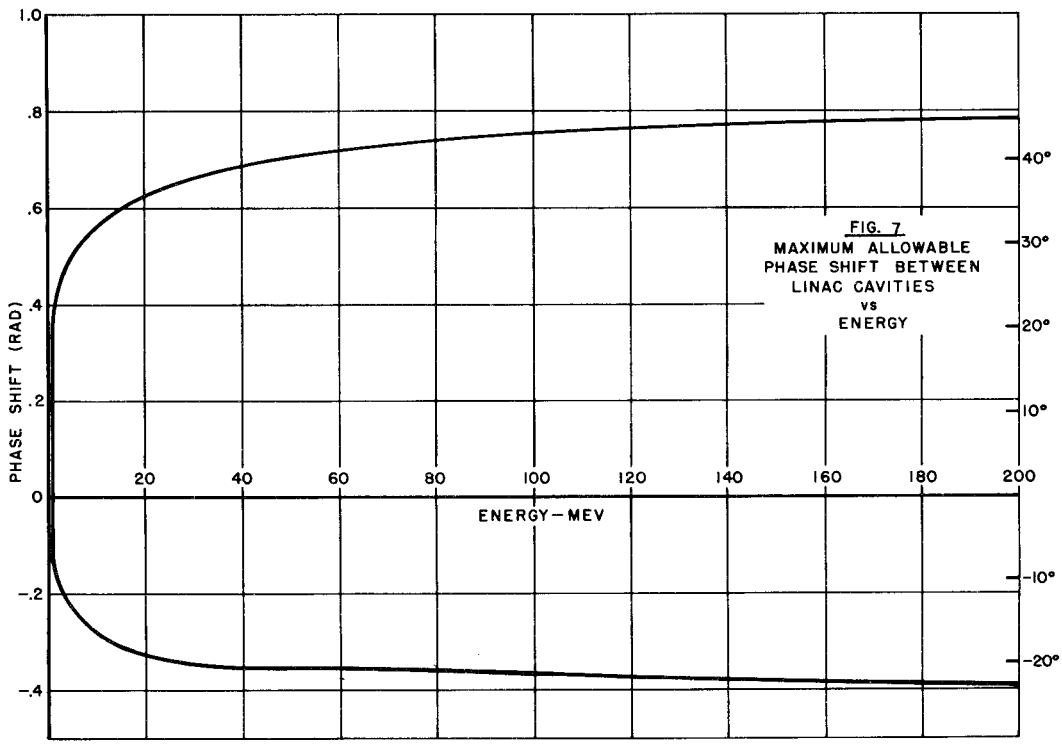

FIG. 7
MAXIMUM ALLOWABLE PHASE SHIFT BETWEEN LINAC CAVITIES
vs
ENERGY

The rf system, shown in Fig. 5, will consist of seven rf power amplifiers (PA's), one for each of the linac cavities. Each PA will use a single RCA 7835 super-power triode rated at 5 MW peak power and will be driven by an amplifier chain, capable of supplying approximately 160 kW peak drive power. The amplifier chains will be excited by a single low level oscillator-amplifier system so that all final amplifiers will be driven at a single frequency and at controllable relative phase, maintained by fast servo systems at the low level amplifier stages. This arrangement will permit independent testing of each of the rf amplifier systems and of the cavity it drives. It will also preclude interaction between one PA system and any other. Thus, from the standpoint of tune up and trouble diagnosis, this system will be most versatile. By eliminating interactions at the high power levels, it will be more reliable than with high level coupling.

A separate amplifier chain will drive the buncher and debuncher in order to avoid the effect of beam loading interactions on the amplitude and phase of these cavities.

It is proposed in the new system to use the same scheme that is presently in use on the 50 MeV linac in maintaining frequency stability; i.e., the rf system will be driven from an oscillator until the rf level in the linac cavity reaches approximately the accelerating gradient. At this time, a signal from No. 1 cavity will be gated on in place of the oscillator so that the No. 1 cavity will thereafter be driven at its resonant frequency. All other cavities would be driven at this same frequency, and all would, of course, require very good thermal stability in order to resonate at or near the same frequency, as $\frac{\Delta f}{f} = - \alpha \Delta T$, where α is the coefficient of thermal expansion for the cavity metal.

A further consequence of cavity temperature change is the phase shift resulting from driving a cavity at a frequency different from resonance. The magnitude of this phase shift is proportional to the Q of the cavity, i.e.,

$$\theta \simeq - 2 Q \alpha \Delta T .$$

Figure 6 shows the magnitude of the phase shift as a function of temperature for a few values of Q.

Taking into account the phase damping that can be expected, one can set an upper limit to the magnitude of phase shift between cavities that can be tolerated without loss of particles. As the phase damping is proportional to $\beta^{-3/4}$ one finds that the maximum allowable phase shift varies with energy, as shown in Fig. 7.

This in conjunction with Fig. 6 indicates that cavity temperature stability must be good to $\pm$ 0.25° C in order not to spill particles from the phase bucket in successive cavities. Considering energy spread and other factors, the thermal stability must be very much better than this.

The shape of the curves in Fig. 7 suggests that, since there is still considerable phase damping after the 10 MeV region, it would be desirable to design the first cavity of the linac for 20 MeV or even higher energy. In the ANL case, since we propose to use identical amplifier systems for each of the linac cavities, it will be advantageous to design the first cavity for 20 MeV or more in order to reserve more rf power for the remaining cavities. These are the two main reasons for designing the first cavity for 20 MeV rather than 10 MeV.

SYMON: I didn't see why this diagram that you have here really shows what the tolerance is on the phase shift. If you had one single phase shift that occurs, then I can see that this diagram is relevant, but if you suddenly jump the rf phase, then the packet moves over to where you have shown. If that situation lasts for on the order of a phase oscillation, you have smeared the packet around the boundary so that you no longer can tolerate another jump in phase. The packet is now equal to the full bucket size.

PERRY: Yes, what I showed on the curve was the maximum phase shift.

SYMON: Yes, but it would seem to me that what you are really interested in is a series of small phase errors from tank to tank, which occur at intervals that are short compared to a phase oscillation. Then I don't see that the diagram that you have drawn is relevant.

PERRY: In the case of which you are speaking, it is true, it is not relevant. I was looking only at the maximum phase shift allowable due to frequency shift or temperature change between the first and any successive cavity without loss of particles. This essentially places a maximum tolerance on frequency control or cavity temperature stability. The maximum allowable temperature variation of any cavity would be $\pm$ 0.25°C just to prevent particle spill, and in order to keep the phase spread, and thus the energy spread, to a minimum the temperature stability would have to be very much better than that.

REFERENCES

1. Expected Beam Intensities of the FFAG and ZGS Accelerators, Report to the Atomic Energy Commission of the Ad Hoc Committee, July 31, 1963.

2. Young, D. E. and Austin, B., "Design Study of 200 MeV Injector for ZGS," MURA Technical Note TN-469, April 7, 1964.